Bridge Condition Evaluation by *In Situ* Dynamic Data

A. Alvandi[*,1], J. Bastien[1], C. Cremona[2] and M. Jolin[1]

[1]*Research Center on Concrete Infrastructures (CRIB), Department of Civil Engineering, Université Laval, Québec (Québec), G1V 0A6, Canada*

[2]*Laboratoire Central des Ponts et Chaussées, 58 Bd. Lefebvre, 75732 Paris, France*

Abstract: The performance of vibration-based damage identification techniques for current condition evaluation of existing bridges is studied through their application to dynamic response of an existing concrete bridge. First, *in situ* dynamic tests were performed and modal parameters (mode shapes and frequencies) were identified. As previous sets of *in situ* dynamic parameters were not available, the reference dynamic parameters were obtained from a finite element model of the bridge. Comparing modal parameters of the finite element bridge model and the *in situ* experimental results through damage identification techniques, the bridge current condition was examined. That evaluation results showed that techniques like strain energy and flexibility curvature present promising results for current condition evaluation of existing bridges.

INTRODUCTION

Civil infrastructures begin to deteriorate as soon as they are in service. Maintaining safe and reliable civil infra-structure for daily use is a topic that has received considerable attention in literature in recent years. Most of the current damage detection methods are either visual or localized experimental methods such as acoustic, ultrasonic, magnetic field and radiographic methods. For now, no current experimental method is general enough to be applicable to all the different portions of a structure as they have their own applicability limitations. Moreover, they often require that the location of the damage be known *a priori* and that the portion of the structure being inspected to be readily accessible. Subjected to such limitations, these methods generally detect damage on or near the surface of the structure. The need for more global damage detection methods that overcome the above limitations and which can be applied to complex structures has led to the development of methods that examine variations in the vibration characteristics of the structure. Over the past 30 years, detecting damage in a structure from modifications in dynamic parameters has received considerable attention. The basic premise of global damage detection is that modal parameters, notably natural frequencies and mode shapes are the functions of the physical properties of the structure (mass, damping and stiffness). Therefore, variations in physical properties (stiffness or flexibility) will cause modifications in modal properties. In damage detection, the modal properties most commonly used are eigenfrequencies and mode shapes. Early attempts to use frequency shifts to detect and localize damage include those by Vandiver 1975 [1], 1977 [2] and Adams *et al*. 1978 [3].

At about the same time, researchers started using mode shape changes for damage detection purposes (West 1984 [4], Yuen 1985 [5]). Since then, many techniques have been developed using frequency and mode shape variations to locate and quantify damage. These techniques have been well documented in the extensive literature reviews, published by Siddique *et al*. 2007 [6], Zhou *et al*. 2007 [7], Doebling *et al*. 1996 [8] and Salawu 1997 [9]. A major limitation of such damage detection techniques is that, frequency shift and mode shape variation are generally not very sensitive for local and moderate level of damages. The somewhat low sensitivity of these parameters requires either very precise measurement or large levels of damage. Tests conducted on the I-40 Bridge (Farrar *et al*. 1994 [10]) have also demonstrated this point. Pandey *et al*. 1991 [11] proposed using curvature mode shapes as a means of locating structural damage. In their research, curvature mode shape was shown to locate damages adequately, in cases where traditional damage localization techniques, such as the Coordinate Modal Assurance Criterion - COMAC (West 1984), had failed. Although vibration-based damage identification techniques have been used successfully in a number of cases (Doebling and Farrar 1998 [12]), there are still some limitations associated with their application for current condition evaluation of existing bridges. In fact, in North America it is common knowledge that a significant number of bridges is old and requires repairing or strengthening. In most cases, the *in situ* dynamic properties of these bridges can be registered, but seldom is a previous set of records available for comparison purposes (reference state). Furthermore, the original (undamaged) state of these existing bridges is even more rarely available since it is not common practice to assess dynamic properties of new structures.

At first, this article presents a quick review of existing vibration-based damage identification techniques. In order to evaluate the efficiency of these techniques for bridge condition evaluation, a numerical model of an existing concrete bridge is presented and some damage scenarios are introduced into it. Following the discussion regarding the performance of these techniques, the most efficient ones will be

*Address correspondence to this author at the Research Center on Concrete Infrastructures (CRIB), Department of Civil Engineering, Université Laval, Québec (Québec), G1V 0A6, Canada;
E-mail: alireza.alvandi@gci.ulaval.ca

1874-8376/08

applied to the *in situ* dynamic data of an existing bridge for current condition evaluation.

VIBRATION-BASED DAMAGE IDENTIFICATION TECHNIQUES: A REVIEW

In this section, some current vibration-based damage identification techniques will be reviewed. In practice, due to the difficulty involved in exciting the higher modal frequencies (need of high quantity of energy) of a structure, the techniques selected herein require only a small number of mode shapes and/or frequencies.

Mode Shape Curvature

In formulating the eigenvalue problem, Pandey *et al*. 1991, assumed that structural damage affects only the stiffness matrix and not the mass matrix. For the undamaged condition the eigenvalue problem is expressed as:

$$\left(\left[K\right]-\lambda_i\left[M\right]\right)\left\{\Phi_i\right\}=\left\{0\right\} \tag{1}$$

where $\left[K\right]$ and $\left[M\right]$ are respectively the stiffness and mass matrices, λ_i and $\left\{\Phi_i\right\}$ are the i^{th} eigenvalue and the i^{th} eigenvector. Similarly, the eigenvalue problem for the damaged condition is:

$$\left(\left[K^*\right]-\lambda^*_i\left[M\right]\right)\left\{\Phi^*_i\right\}=\left\{0\right\} \tag{2}$$

where the asterisks identify the stiffness matrix, the i^{th} eigenvalue, and the i^{th} eigenvector of the damaged structure. The pre- and post-damage eigenvectors are the basis for damage detection. Mode shape curvature of a beam in the damaged and undamaged condition can then be estimated numerically from the displacement mode shapes. In the case of a beam, given the damaged and undamaged mode shapes, and considering a beam cross section at location x subjected to a bending moment $M\left(x\right)$, the curvature at location x, $v''\left(x\right)$, is given by:

$$v''\left(x\right)=\frac{M\left(x\right)}{EI} \tag{3}$$

where E is the modulus of elasticity and I the moment of area of the section. Thus, for a given bending moment applied to the damaged and undamaged structure, a reduction of stiffness associated with a damage will in turn, lead to an increase in curvature. Zhou *et al*. 2007 proposed direct application of *in situ* measured curvature for damage detection. In fact, using this approach improves detection precision by reducing some numerical inherited errors. Reynders *et al*. 2005 [13], comparing experimental and numerical modal curvature of an existing bridge in different sections, show that, the average variation can reach upto 14%. It is to notify that, the experimental number of measurement points has an important impact on the aforementioned variation. The authors would like to add that, for hyperstatic structures like certain bridges, the load redistribution due to local damage could also lead to a bending moment reduction in the damaged area. In this case, depending on the rigidity reduction due to the damage and bending moment redistribution, the curvature could decrease or increase.

Flexibility Matrix

Another type of damage identification methods uses the dynamically measured flexibility matrix to estimate modifications in the static behaviour of the structure (Pandey and Biswas 1994 [14]). Because the flexibility matrix is defined as the inverse of the static stiffness matrix, the flexibility matrix F relates the applied static force f and resulting structural displacement u as:

$$\left\{u\right\}=\left[F\right]\left\{f\right\} \tag{4}$$

The expression of the flexibility matrix is written as:

$$\left[F\right]=\left[\Phi\right]\left[\Omega\right]^{-1}\left[\Phi\right]^T=\sum_{i=1}^{n}\frac{1}{\omega_i^2}\left\{\Phi_i\right\}\left\{\Phi_i\right\}^T \tag{5}$$

$\left[\Phi\right]=\left[\left\{\Phi_1\right\},\left\{\Phi_2\right\},...,\left\{\Phi_n\right\}\right]$ is the mode shapes matrix, $\left\{\Phi_i\right\}$ being the i^{th} mode shape. The diagonal matrix of rigidity: $\left[\Omega\right]$ correspond to $\left[\omega_i^2\right]$, where ω_i is the i^{th} frequency. $\left[F\right]$ is the flexibility matrix. Thus, each column of the flexibility matrix represents the displacement pattern of the structure associated with a unit force applied at the associated degree of freedom. Measuring the flexibility matrices before and after damage, the variation matrix $\left[\Delta\right]$ can be obtained:

$$\left[\Delta\right]=\left[F^*\right]-\left[F\right] \tag{6}$$

where, $\left[F\right]$ and $\left[F^*\right]$ are flexibility matrices before and after damage respectively. Now, for each column of matrix Δ, let $\bar{\delta}_j$ be the absolute maximum value of the elements in the j^{th} column. Hence:

$$\bar{\delta}_j=\max\left|\delta_{ij}\right|,\quad i=1,...n \tag{7}$$

where δ_{ij} are the elements of matrix Δ and represent the flexibility variation in each degree of freedom. The column of the flexibility matrix corresponding to the largest $\bar{\delta}_j$ is indicative of the degree of freedom where the maximum variation in flexibility has been produced or where damage could be expected. It should be mentioned that, in this approach the non-linear behaviour of the structure is not considered.

Flexibility Matrix Curvature

By combining certain aspects of the mode shape curvature and the flexibility matrix, Zhang and Aktan (1995) [15] developed an alternative damage detection scheme. Similarly to the mode shape curvature method, the basic concept of this approach is that a localized loss of stiffness will produce a curvature variation at these areas. However, variation in curvature is obtained from the flexibility instead of the mode

shapes. The flexibility matrices, before and after damage can be approximated by the modal parameters:

$$\left[F\right]=\left[\left\{F_1\right\}\left\{F_2\right\}...\left\{F_n\right\}\right]\approx\left[\Phi\right]\left[\Omega\right]^{-1}\left[\Phi\right]^T \quad (8)$$

and

$$\left[F^*\right]=\left[\left\{F_1^*\right\}\left\{F_2^*\right\}...\left\{F_n^*\right\}\right]\approx\left[\Phi^*\right]\left[\Omega^*\right]^{-1}\left[\Phi^*\right]^T \quad (9)$$

where, the asterisks designate the damaged structure. F_1 through F_n (with and without the asterisk) correspond to columns of the flexibility matrix. Zhang and Aktan, used the variation in curvature of the flexibility matrix to determine the location of the damage. The curvature variation is evaluated as follows:

$$\left[\Delta\right]=\sum_{i=1}^{n}\left|\left\{F_i^*\right\}''-\left\{F_i\right\}''\right| \quad (10)$$

where $\left[\Delta\right]$ and n represent respectively, the absolute curvature variation and the number of the degree of freedom (or identified number of mode shapes).

Strain Energy (Damage Index)

Considering the flexural rigidity about axis z of the three-dimensional beam of the type Bernoulli-Euler of length *L* (Fig. **1**), the strain energy can be expressed as (Cornwell *et al*. 1999 [16]):

$$U=\frac{1}{2}\int_0^L EI_z(x)\left(\frac{\partial^2 y}{\partial x^2}\right)^2 dx \quad (11)$$

For simplicity purposes EI_z being replaced by EI, the strain energy associated to a given mode shape ϕ_i is:

$$U_i=\frac{1}{2}\int_0^L EI(x)\left(\frac{\partial^2\phi_i}{\partial x^2}\right)^2 dx \quad (12)$$

Assuming that the beam is divided in *N* elements, the strain energy of an element for a given mode shape may therefore be expressed as:

$$U_{ij}=\frac{1}{2}\int_{a_j}^{a_{j+1}} EI(x)\left(\frac{\partial^2\phi_i}{\partial x^2}\right)^2 dx \quad (13)$$

with a_j, a_{j+1} delimiting the element *j*. Based on the strain energy related to each element and the strain energy of the complete structure for a given mode, the fractional strain energy F_{ij} may be defined. For a beam-like structure, F_{ij} is the ratio between an element and beam strain energy.

$$F_{ij}=U_{ij}/U_i \quad (14)$$

with $\sum_{j=1}^{N}F_{ij}=1$, where *N* is the number of elements. Similar expressions can be derived for a damaged beam-like structure:

$$F_{ij}^*=U_{ij}^*/U_i^*;$$

$$U_i^*=\frac{1}{2}\int_0^L EI^*(x)\left(\frac{\partial^2\phi_i^*}{\partial x^2}\right)^2 dx; \quad (15)$$

$$U_{ij}^*=\frac{1}{2}\int_{a_j}^{a_{j+1}} EI^*(x)\left(\frac{\partial^2\phi_i^*}{\partial x^2}\right)^2 dx$$

In the presence of low rate modifications, a first order approximation can be drawn:

$$F_{ij}^*=F_{ij}+\text{higher order terms} \quad (16)$$

leading to:

$$1=\frac{F_{ij}^*}{F_{ij}}=\frac{U_{ij}^*U_i}{U_{ij}U_i^*}=\frac{\int_{a_j}^{a_{j+1}}EI^*(x)\left(\frac{\partial^2\phi_i^*}{\partial x^2}\right)^2 dx}{\int_{a_j}^{a_{j+1}}EI(x)\left(\frac{\partial^2\phi_i}{\partial x^2}\right)^2 dx}\frac{\int_0^L EI(x)\left(\frac{\partial^2\phi_i}{\partial x^2}\right)^2 dx}{\int_0^L EI^*(x)\left(\frac{\partial^2\phi_i^*}{\partial x^2}\right)^2 dx} \quad (17)$$

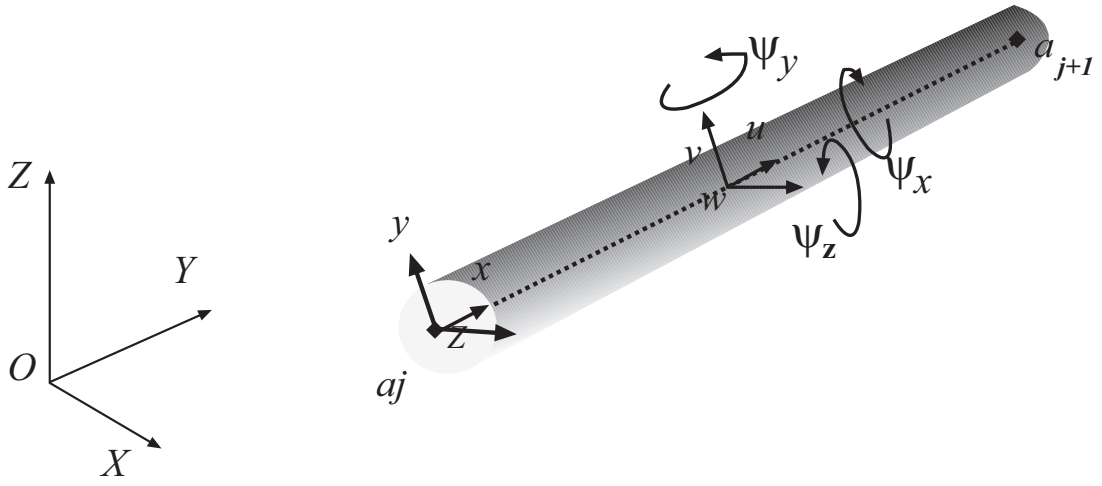

Fig. (1). Three-dimensional beam element.

Fig. (2). Elevation view of the concrete bridge.

After simplification and taking the mean of a set of *n* mode shapes, this last equation can be re-written as:

$$\beta_j = \frac{\widehat{EI}_j}{\widetilde{EI}_j^*} = \frac{1}{n}\sum_{i=1}^{n} \frac{\int_{a_j}^{a_{j+1}} \left(\frac{\partial^2 \phi_i^*}{\partial x^2}\right)^2 dx}{\int_{a_j}^{a_{j+1}} \left(\frac{\partial^2 \phi_i}{\partial x^2}\right)^2 dx} \frac{\int_0^L \left(\frac{\partial^2 \phi_i}{\partial x^2}\right)^2 dx}{\int_0^L \left(\frac{\partial^2 \phi_i^*}{\partial x^2}\right)^2 dx} \quad (18)$$

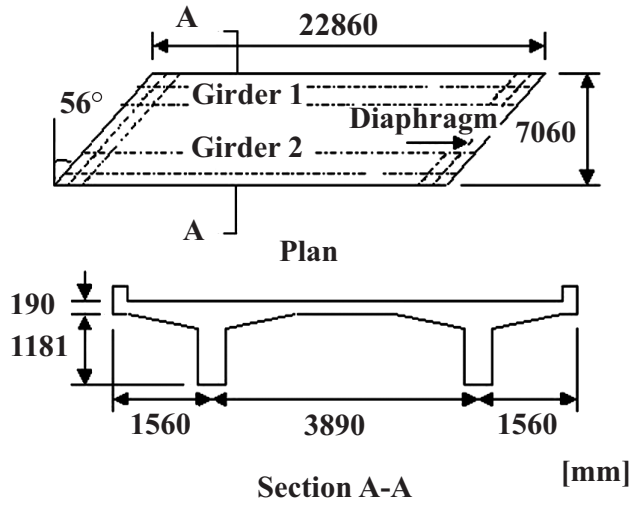

Fig. (3). Geometry and cross-section of the bridge.

This expression slightly differs from the one introduced in Cornwell *et al*. 1999. β_j is the damage index for element *j*. In order to generalize damage index and be independent of a structure type, a normalized damage index is often preferred and may be expressed as:

$$z_j = \left(\beta_j - \bar{\beta}\right)/\sigma_\beta \quad (19)$$

where $\bar{\beta}$ and σ_β are the mean and standard deviations of the sample values β_j. Lets us recall that z_j does not represent a damage extend. but the confidence for the presence of a damage. If we assume that z_j is a standard normal variable, using the normal distribution rule, it can be proved that $\Phi\left(z_j\right)$ is the confidence level to have detected a damage in element *j* (Φ being the probability function of the standard normal variable). For example, 95% confidence level is achieved, consequently for $z_j \approx 1.65$. More detail about probability functions can be found in Cornwell *et al*. 1999 and Alvandi and Cremona 2002 [17]. Li *et al*. 2006 [18] presented a decomposition method based on modal strain energy. Using this technique, both transversal and axial mode shapes are considered. Further more, Hu *et al*. 2006 [19] proposed a modified strain energy method that could be applied directly to damaged mode shapes. As further development for practical application of these techniques is needed, they are not used in this study.

Modal Assurance Criterion (MAC)

A Modal Assurance Criterion (MAC) sometimes referred to as a modal correlation coefficient is calculated to quantify the correlation between two mode shapes (Allemang and Brown 1982 [20]). Let us suppose that $\left[\Phi_A\right]$ and $\left[\Phi_B\right]$ are matrices made-up of m_A and m_B mode shapes measured in *n* measurement points. These are thus matrices of dimension $n \times m_A$ and $n \times m_B$. For the $i = 1,2,...m_A$ and $j = 1,2,...m_B$ mode shapes, the MAC is defined as:

$$MAC_{ij} = \frac{\left|\sum_{k=1}^{n} \left(\Phi_A\right)_k^i \left(\Phi_B\right)_k^j\right|^2}{\sum_{k=1}^{n} \left(\left[\Phi_A\right]_k^i\right)^2 \sum_{k=1}^{n} \left(\left[\Phi_B\right]_k^j\right)^2} \quad (20)$$

where, $\left[\Phi_A\right]_k^i$ and $\left[\Phi_B\right]_k^j$ are the k^{th} component of mode shapes $\left[\Phi_A\right]^i$ and $\left[\Phi_B\right]^j$. The MAC coefficient presents the correlation degree between i^{th} and j^{th} mode shapes in *A* and *B,* and it varies between 0 and 1. For the identical mode shapes, a scalar value of one is calculated. In this study, this coefficient is presented in percentage, i.e. 0 to 100 percent.

RESEARCH OBJECTIVES

The objectives of the current research are to study the performance of the vibration-based damage identification techniques and their application for current condition evaluation of existing bridges. These objectives will be studied through experimental and numerical data of an existing concrete bridge. In order to compare the performance of these techniques, some damage scenarios were defined in the finite element model of the bridge. Having numerical and experimental modal parameters obtained respectively by finite element model and *in situ* dynamic test, the current condition of the bridge can be evaluated. It is to notify that, in this study, the effect of non-linearity on dynamic response is not considered. More information regarding these non-linearities can be found in Rudenko 2006 [21].

BRIDGE DESCRIPTION

The single span concrete bridge under study was constructed in 1944 in the province of Quebec, Canada (Fig. **2**). This concrete bridge is composed of two T-beams connected by an upper slab 190 mm thick and two diaphragms (Fig. **3**). The bridge has a span length of 22.86 m, and a width of 7.0 m with a skew of 56°. The two diaphragms of 350 mm by 600 mm are situated at each girder's extremity. A first estimate of the bridge loading capacity, assessment based on a simplified method proposed by the Canadian Highway Bridge Design Code (CHBDC 2000 [22]), showed that the bridge was not able to carry the current legal maximum load (Jolin *et al*. 2003 [23]).

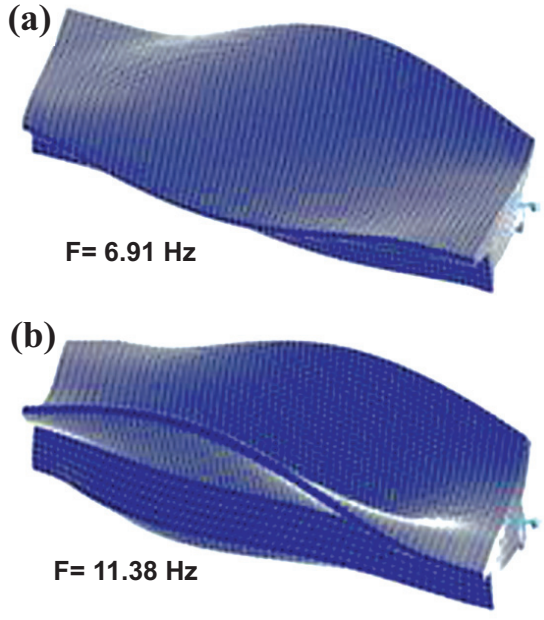

Fig. (4). Finite element mode shapes and frequencies: (**a**) torsional (**b**) bending.

This situation arises mainly because the design loads used in the 1940's, were much lower in magnitude than the ones being considered today. Therefore, considering the above and all relevant inspection information, authorities submitted the bridge to a monitoring programme in 2002, until its replacement in 2006.

Table 1. Finite Element Frequency Variations

Damage Scenarios	Mode 1	Mode 2
Initial	6.91	11.38
Damage in the northern beam (10%)	6.90	11.38
Variation (%)	0.10	0.00
Damage in the northern beam (50%)	6.85	11.37
Variation (%)	0.61	0.054
Damage in the deck (10%)	6.91	11.36
Variation (%)	0.00	0.10
Damage in the deck (50%)	6.84	11.02
Variation (%)	0.70	1.96
[Unit : Hz]		

PERFORMANCE OF THE VIBRATION-BASED DAMAGE IDENTIFICATION TECHNIQUES

Numerical Model of the Bridge

A finite element model of the bridge was developed and analysis was performed in the *ANSYS* finite element environment. Deck, girders and diaphragms were modeled using *SOLID45*, eight nodded brick elements (ANSYS 2007 [24]). In order to quantify the material properties, nine cores were taken from the deck, girders and diaphragms. According to these results, the mean value of the compressive strength of concrete was 42 MPa in the girders and diaphragms, and 35 MPa in the deck. These values were introduced as one of the concrete material properties in the finite element model. A density of 2400 kg/m³, a Poisson ratio of 0.2, and Young's modulus of 32000 MPa (beam) and 29000 MPa (deck and diaphragm) were also considered for the concrete. Modal analysis was realized with the Lanczos block for the eigenvector extraction method in the ANSYS environment. The first two numerical mode shapes and frequencies identified in torsion and bending are shown in Fig. (**4**).

Numerical Damage Scenarios

To demonstrate the detection potential of the presented vibration-based damage identification techniques, two damage scenarios were introduced at two different parts of the bridge: (1) in the northern beam, (2) in the middle of the deck. For the first scenario, some element rigidities situated at the northern beam centre were reduced to 10, and 50% of their original values (Fig. **5a**). In the second scenario, the rigidity of the selected elements in the deck centre was reduced to 10, and 50% of their original values (Fig. **5b**).

Detection Results

In this section, the damage identification techniques will be applied to the first two mode shapes and frequencies of the structure before and after each numerical damage scenario. In the case of the strain energy method, the plate-like elements were considered (Cornwell *et al*. 1999). For each method, the detection results were based on undamaged and

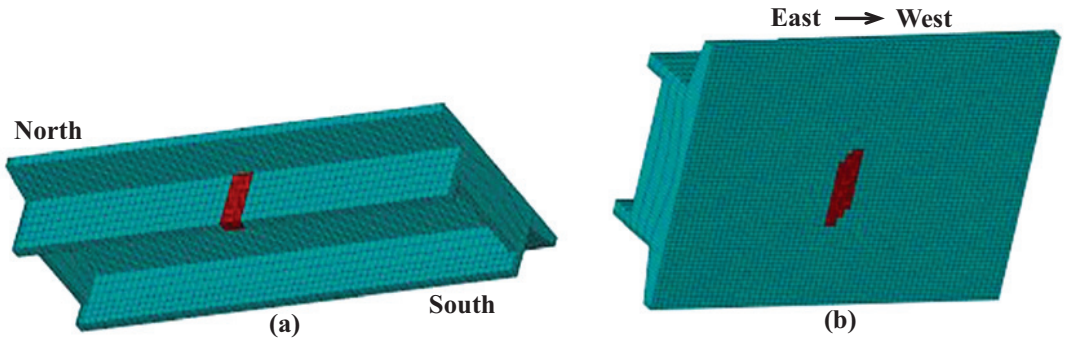

Fig. (5). Damage scenarios: (**a**) damage in the northern beam, (**b**) damage in the deck.

damaged mode shapes and frequencies measured at three measurement lines, which were later used for the *in situ* dynamic test (Fig. **10**). For demonstration purposes, the final results were obtained by longitudinal and transversal interpolation of the measuring points on the deck surface. The frequency variations before and after each damage scenario are given in Table **1**. Fig. (**6**) presents the detection results of the first damage scenario (related to a 50% damage in the northern beam).

According to this figure, all the methods were able to detect the damaged zone located at the centre of the northern beam. However, the mode shape curvature method and the flexibility curvature method exhibited some false detections in or close to the bridge extremities (Fig. **6a**,**c**). This phenomenon did not occur with the strain energy method which properly localized the damaged zone (Fig. **6d**). The detection results for the same scenario with a 10% damage are shown in Fig. (**7**). In this case, the introduced damage intensity (10% rather than 50%) influenced the results magnitude but did not have any impact on the damage location identification. The detection results for the second scenario with a 10% damage are shown in Fig. (**8**). For this damage scenario, all methods were able to localize the introduced modifications in the deck centre portion. As similar trends were obtained for the second scenario with a 50 percent damage,

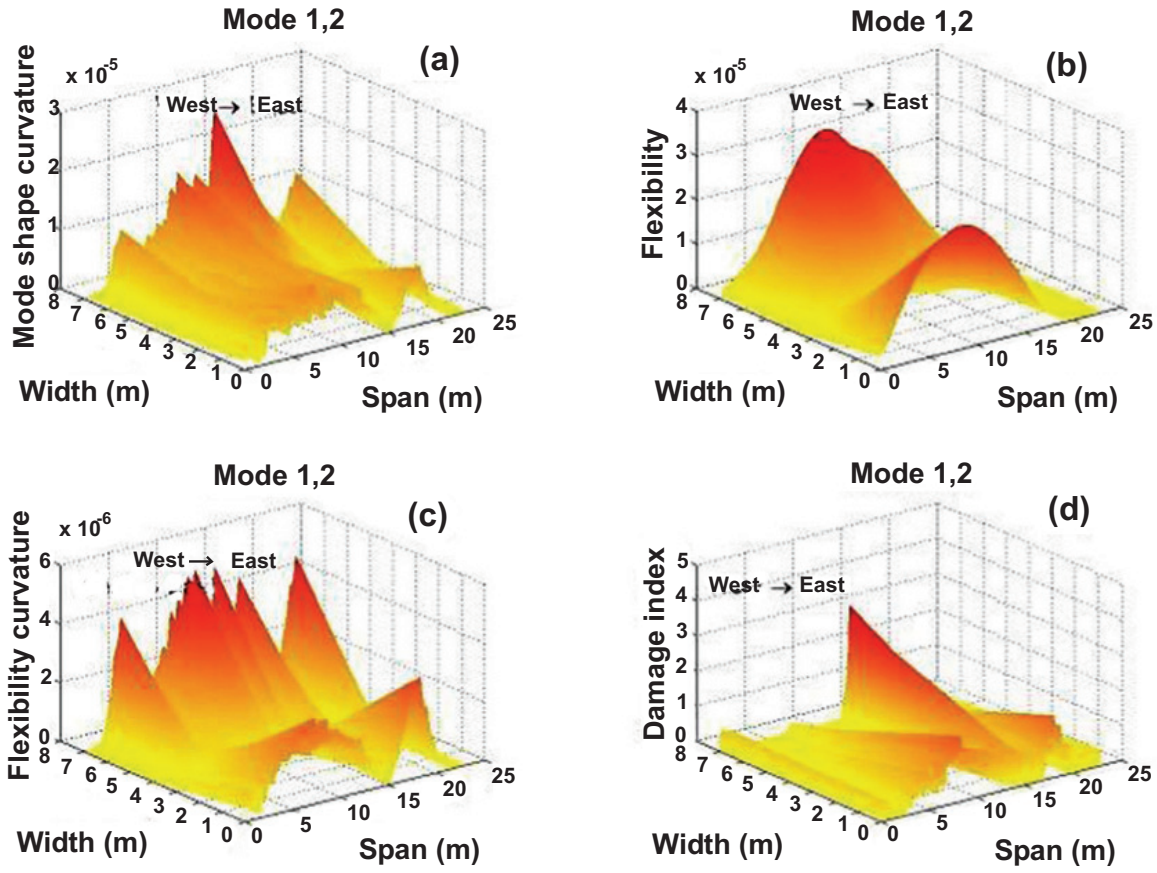

Fig. (6). Detection results for 50% damage in the northern beam according to: (**a**) mode shape curvature; (**b**) flexibility; (**c**) flexibility curvature; (**d**) strain energy methods.

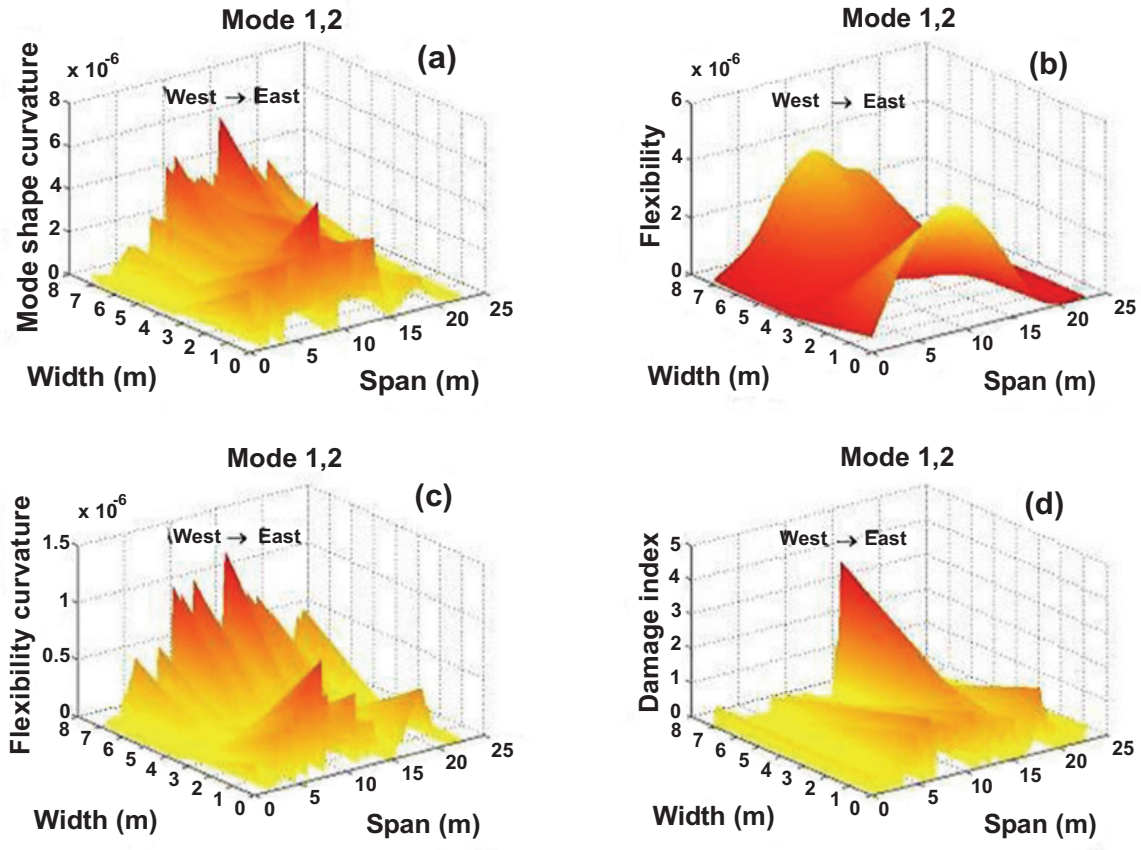

Fig. (7). Detection results for 10% damage in the northern beam according to: (**a**) mode shape curvature; (**b**) flexibility; (**c**) flexibility curvature; (**d**) strain energy methods.

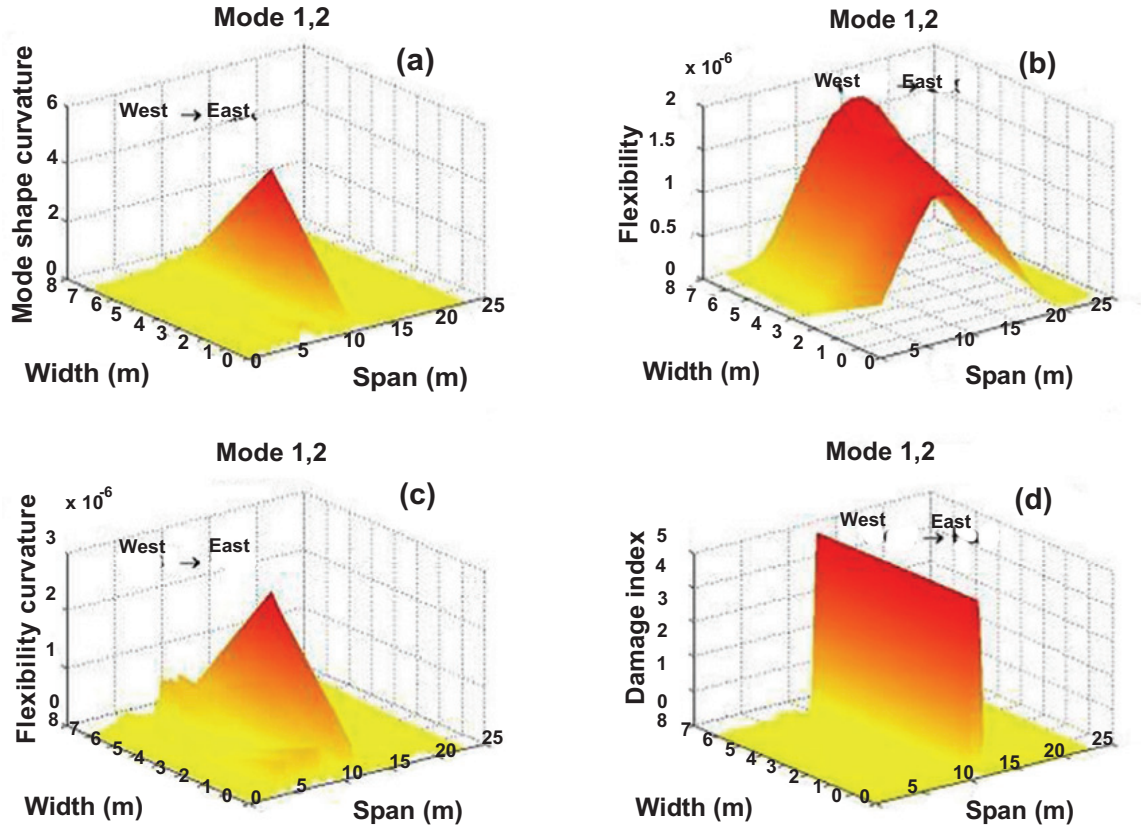

Fig. (8). Detection results for 10% damage in the deck according to: (**a**) mode shape curvature; (**b**) flexibility; (**c**) flexibility curvature; (**d**) strain energy methods.

the results were not presented herein. As seen previously, for the first damage scenario, the mode shape curvature method and the flexibility curvature method (Fig. **6a**,**c** and Fig. **7a**,**c**), detect damage at different locations along the north beam (rather than at its central portion only) and, in some cases, along the southern bridge beam. On the other hand, methods like the strain energy showed stability and consistency in detecting the relevant damage location.

CURRENT CONDITION EVALUATION OF THE BRIDGE

In Situ Dynamic Test

There are two main types of dynamic tests for bridges: forced vibration and ambient vibration. In general, in the forced vibration technique, the structure is excited artificially, by the sudden drop of a load on it (shakers or drop weights) and a condition of free vibration is induced. In contrast, ambient vibration testing uses traffic generally, as the excitation source. More information about bridge excitation methods can be found in Farrar *et al*. 1999 [25] and Cremona *et al*. 2003 [26].

In this study, two predefined trucks were used as a source of vibration. A series of vibration tests were conducted on July 4th, 2004 by the Quebec Ministry of Transportation. As the traffic was not so intense, the bridge was closed occasionally, and the two trucks were able to cross the structure one after the other (Fig. **9**). The total mass of each truck was 25650 and 25900 kg respectively. The driving speeds of each truck were 50 and 70 km/h in both directions.

Instrumentation Plan

The response of the bridge was measured by eight vertical and four horizontal (transversal) accelerometers, which were placed under the girders and the slab of the bridge. As the number of sensors was not sufficient to measure the behaviour of the entire bridge at once, three set-ups with two reference points in each set-up were considered.

Fig. (9). Trucks used for bridge excitation.

Fig. (**10**) presents one of these set-ups. where letters Z and Y refer to the vertical and horizontal accelerometers. The uniaxial force balance accelerometers commercially known as EpiSensor ES-U were used.

Table 2. Frequency Variations: Finite Element (Before and After Boundary Condition Correction (BCC)) and Experimental

Mode	Frequency (Hz)			
	Finite Element		Experimental	Variation (%)
	Before BCC	After BCC		
1	6.91	7.87	7.66	2.67
2	11.38	12.63	12.43	1.58

Table 3. Modal Assurance Criterion (MAC), Before and After Boundary Condition Correction (BCC)

Measurement Line	MAC (%)			
	Before (BCC)		After (BCC)	
	Mode 1	Mode 2	Mode 1	Mode 2
Line1	98.25	80.57	98.19	82.75
Line2	92.80	86.53	92.70	87.41
Line3	98.74	73.42	98.94	81.29
Average	96.60	80.17	96.61	83.81

Modal Identification

The modal parameters; natural frequencies and mode shapes were extracted from the recorded signals using frequency domain decomposition by the *ARTeMIS* program. A detailed discussion and the theoretical background of this program can be found in Brincker *et al*. 2001 [27] and 2000 [28]. In order to examine the influence of different parameters such as the path and speed of trucks, several dynamic tests were performed on the bridge. All tests were completed in the same day using the same equipment. For each test, the frequencies and mode shapes were obtained with the ARTeMIS program for the portion of the time history, when the two trucks were off the bridge. In this way, the weight of the trucks was excluded from the mass of the bridge. It should be noted that all the three set-ups were used for modal identification. As the variation of frequencies of the different tests was negligible for the required precision in this study (0.013 and 0.014, for the first and second frequencies), the mean values were used for structural evaluation purposes (i.e. 7.66 Hz and 12.43 Hz for the first and second frequencies). The first two mode shapes used corresponded to the mean values of all the identified mode shapes (Fig. **11**).

Boundary Condition Correction (BCC)

Boundary condition correction consists of adjusting the finite element model so it reproduces the actual boundary condition more accurately. In fact, due to some reparations previously done on the bridge, the boundary conditions were modified compared to the initial ones. For this purpose, *in situ* static test data (internal stresses and vertical displacements of the beams) registered two years before the dynamic test were used.

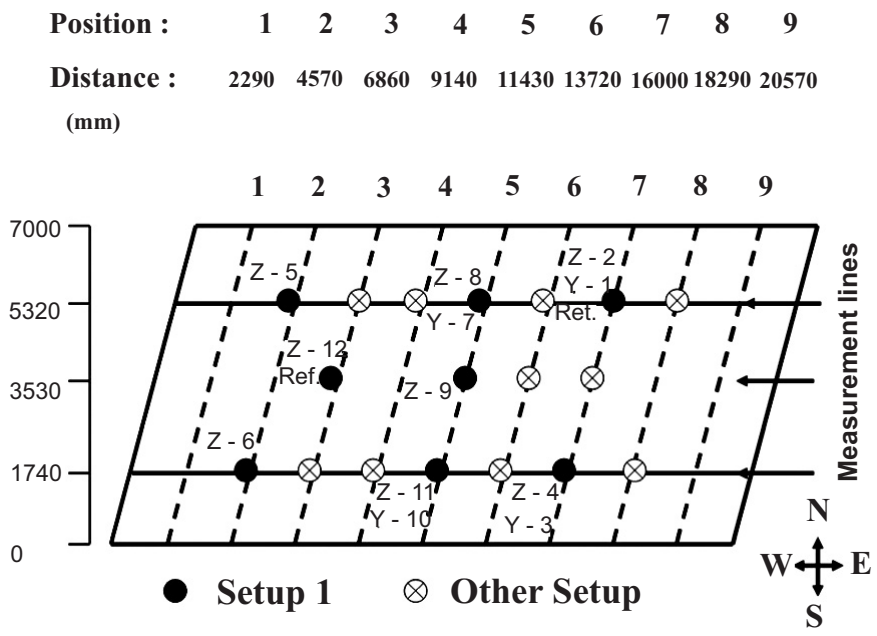

Fig. (10). Accelerometer locations and measurement lines.

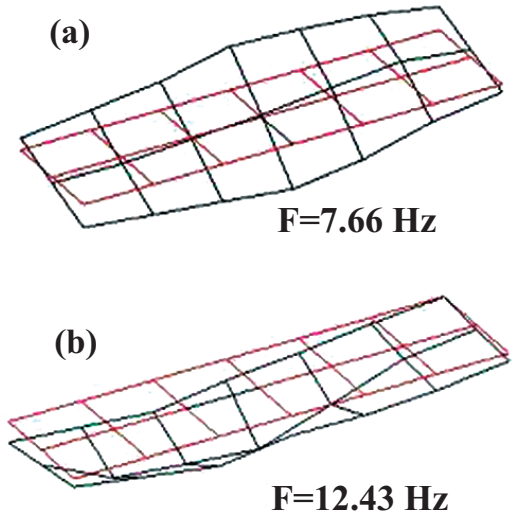

Fig. (11). Experimental mode shapes: (**a**) torsional (**b**) bending.

The static tests consisted in stopping a truck (the same truck used for the dynamic test), in pre-defined positions along with the deck, while monitoring strain and displacement with sensors installed on the structure (Jolin *et al*. 2003). Afterwards, internal stresses and displacements resulting from the static test were compared to the corresponding finite element results. The correction took place only, by adjusting the numerical model boundary conditions only. As example, Fig. (**12**) shows a stress comparison between static tests and numerical results, according to different truck positions along with the deck. Comparison of the numerical model and the static results showed that the restrained boundary conditions in all directions at the bridge extremities enhanced the similitude between results. The comparison between frequencies and the Modal Assurance Criterion (MAC) coefficients of the experimental and finite element model before and after boundary modifications are shown in

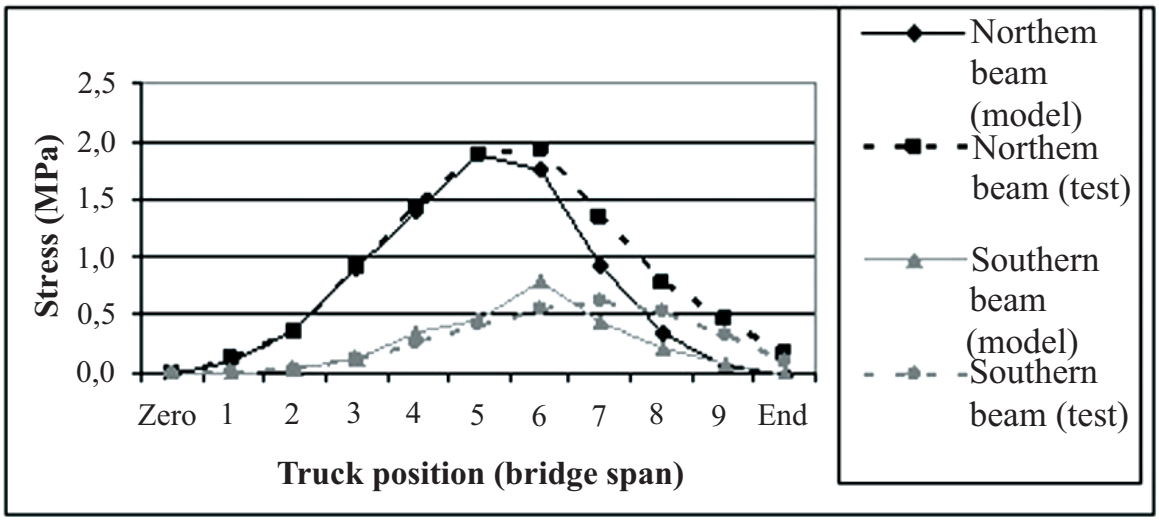

Fig. (12). Comparison of internal stresses (finite element and *in situ* static test).

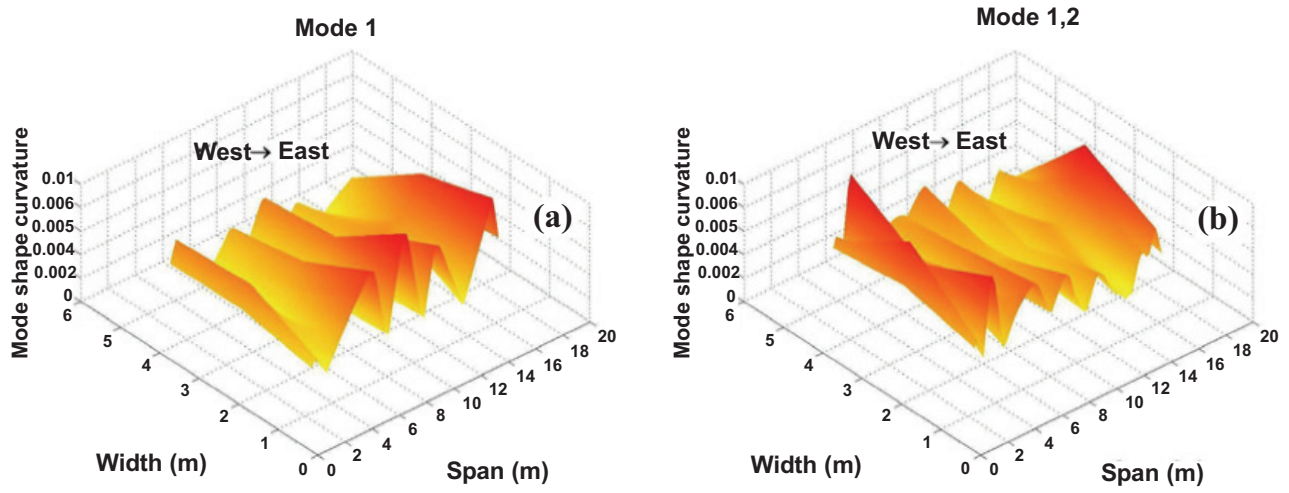

Fig. (13). Detection results of the mode shape curvature method using: (**a**) first mode shape, (**b**) the first two mode shapes.

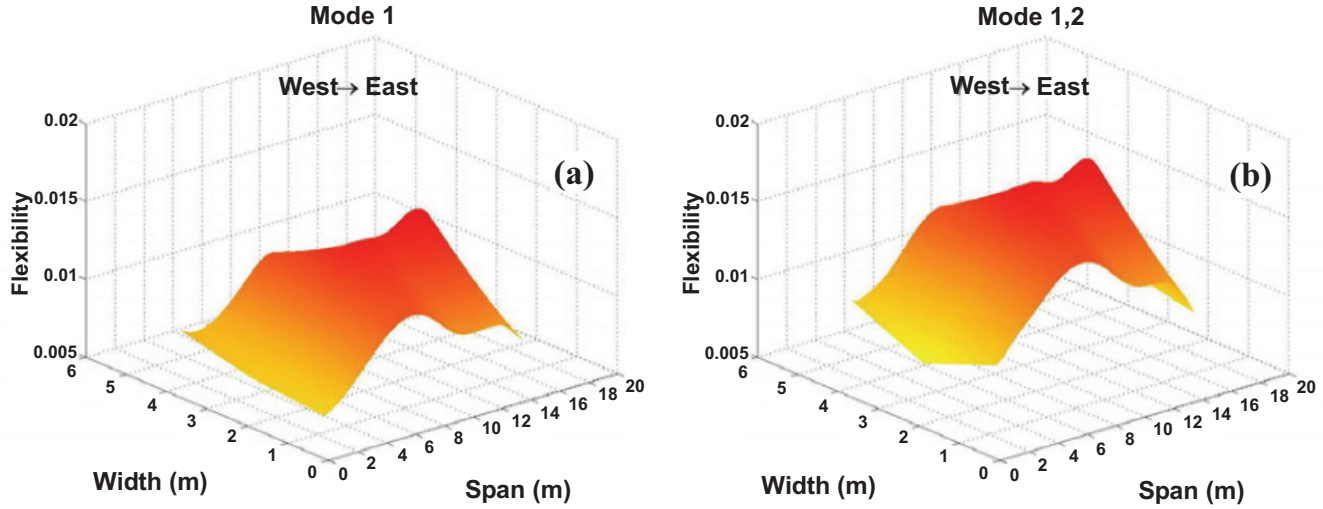

Fig. (14). Detection results of the flexibility method using: (**a**) first mode shape, (**b**) the first two mode shapes.

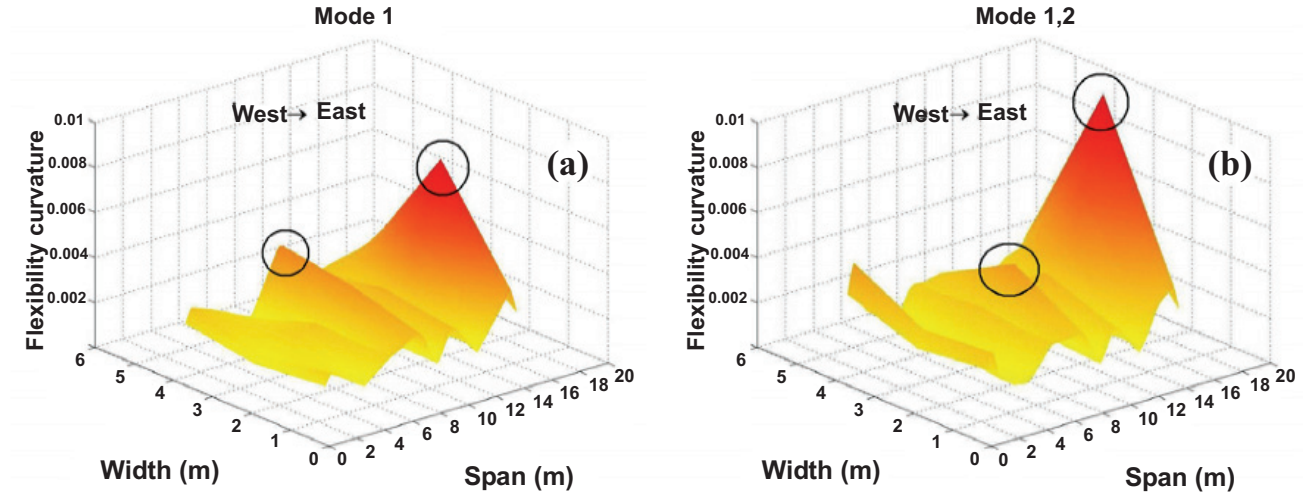

Fig. (15). Detection results of the flexibility curvature method using: (**a**) first mode shape, (**b**) the first two mode shapes.

Tables **2** and **3**. Table **2** reveals that while correction brings the experimental-numerical frequency values closer, there is still a gap which reflects deterioration. In fact, part of these variations could also be due to the numerical model itself. However, for a 60 years old bridge, which was considered negligible compared to the existing deteriorations.

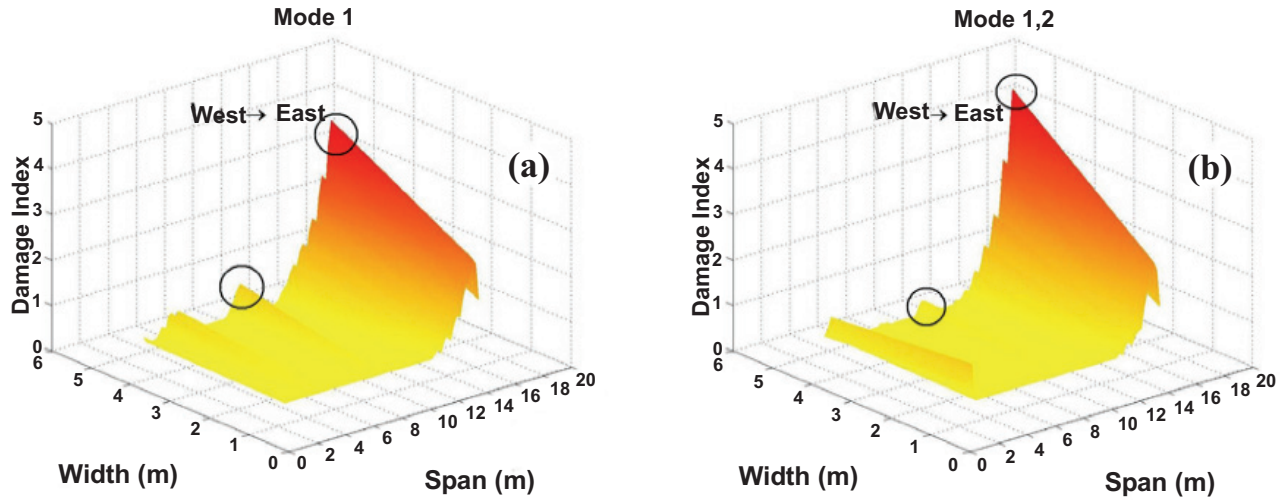

Fig. (16). Detection results of the damage index method using: (a) first mode shape, (b) the first two mode shapes.

Table **3** presents the same trends for the mode shapes. Correction had a larger impact on the MAC criterion for the second mode shape. This improvement regarding the bending mode shape is due to the fact that the restrained boundary conditions better represented the bridge behaviour at the extremities.

Evaluation Results

Comparing experimental and numerical modal parameters (finite element) through vibration-based damage identification techniques, the current condition of the bridge is evaluated. For this purpose, only the first or both first and second mode shapes and frequencies were used. Figs. (**13**) and (**14**) present respectively, the mode shape curvature and flexibility method results. These two methods do not precisely localize a specific damage zone, they rather give an indication that damage is distributed throughout the deck. As far as the flexibility curvature method is concerned, it localizes damage in the centre and eastern part of the bridge (Fig. **15**). The strain energy method confirms the flexibility curvature detection while putting emphasis on the eastern part of the bridge with 99% confidence level ($z_j \approx 4$) as being the most damaged area (Fig. **16**) and providing 63% confidence level for the centre part of the bridge ($z_j \approx 0.35$). It should be mentioned that the above conclusions and findings are not dependent on the choice of the mode selection (first or both first and second shape modes). Even though the MAC coefficient between experimental and numerical data of the second mode was not perfect (87%), it provided results similar to the first mode shape. Considering the findings of the numerical detection results of this paper stating that the strain energy method and the flexibility curvature method seemed the most robust methods and considering the similitude of the detection findings between the flexibility curvature method and the strain energy method (Figs. (**15**) and (**16**)), it can be concluded that the eastern extremity and centre part of the bridge are areas, where damage is expected. Considering the flexibility curvature and strain energy method results, respectively 0.009 flexibility curvature variation compared to 0.002 in Fig. (**15**) and 99% confidence level compared to 63% in Fig. (**16**), it was concluded that the severity and confidence level of having damage in the eastern extremity was much higher than in the centre part of the bridge. These findings are very encouraging and tend to demonstrate that damage identification techniques can be successfully used on existing deteriorated bridges. Here, no reference dynamic data were available and a bridge numerical model provided the needed data. Again, it should be pointed out that the bridge selected for this study is more than 60 years old and had suffered important deterioration. This situation added complexity for establishing the reference numerical bridge model as the bridge had experienced important structural behaviour modification over time (see Table **2**, frequency shift). Here, because of the large time gap, it was decided that the reference bridge model would incorporate boundary condition correction according to the static tests performed on the bridge. By doing so, the damage detection techniques would therefore, give indications of damage other than those associated with the boundary conditions in the bridge extremities. In an ideal situation, it is expected that dynamic data are recorded at regular intervals over a bridge service life period and that reference dynamic data are regularly updated for damage detection technique applications. By doing so, the detected damage is the one appearing and evolving between intervals.

CONCLUSIONS

In this paper, the performance of different damage identification techniques was reviewed through their application to a concrete bridge structure. First, in order to assess the capacity of the different methods to detect a specific damage, a finite element model of the bridge was proposed and different damage scenarios were introduced. The application of damage identification methods to the bridge finite element model (before and after each damage scenario,) revealed that the strain energy method and the flexibility curvature method provided better detection results than the other studied techniques. Secondly, the concrete bridge under study was submitted to *in situ* dynamic testing and the actual bridge modal

parameters were identified. As no reference on experimental dynamic data existed, a finite element model of the bridge was developed and the resulting modal parameters were used as the reference ones. Application of damage identification techniques to the numerical (finite element) and the experimental modal parameters was performed. Once again the strain energy method and the flexibility curvature method were the most successful ones. These results are very promising and demonstrated that global evaluation of structures reveals the most probable damage zones. Once these areas are localized, the local damage detection techniques or detailed inspection can be applied to these areas.

It should be remembered that as the strain energy method does not provide the quantity of the damage, it is essential that its results are compared with the flexibility curvature before final judgment as it was performed herein. Results of the studied bridge structure, demonstrated that the location of damaged areas of existing bridges could be assessed by a simple dynamic test *via* appropriate identification damage techniques. It is also expected that the use of such damage detection techniques could be very useful in tracking damage progression between two dynamic tests and give guidance in the selection of the location to be subjected for detailed inspections.

ACKNOWLEDGEMENTS

The writers would like to gratefully acknowledge the Quebec Ministry of Transportation, especially Marc Savard and Jean-François Laflamme and the Natural Science and Engineering Research Council of Canada for their support and their precious collaboration.

REFERENCES

[1] Vandiver JK. Detection of structural failure on fixed platforms by measurement of dynamic response. Proceeding of the 7th Annual Offshore Technology Conference 1975; 243-252.

[2] Vandiver JK. Detection of structural failure on fixed platforms by measurement of dynamic response. J Petroleum Technol 1977; 305-310.

[3] Adams RD, Cawley P, Pye CJ, Stone BJ. A vibration technique for non-destructively assessing the integrity of structures. J Mechan Eng Sci 1978; 20(2): 93-100.

[4] West WM. Illustration of the use of modal assurance criterion to detect structural changes in an orbiter test specimen. Proceeding of the Air Force Conference on Aircraft Structural Integrity 1984.

[5] Yuen MMF. Numerical study of eigenparameters of a damaged cantilever. J Sound Vibrat 1985; 103(3): 301.

[6] Siddique AB, Sparling BF, Wegner LD. Assessment of vibration-based damage detection for an integral abutment bridge. Can J Civ Eng 2007; (34): 438-452.

[7] Zhou Zhengjie, Wegner Leon D, Sparling BF. Vibration-based detection of small-scale damage on a bridge deck. J Struct Eng ASCE 2007; (133): 1257-1267.

[8] Doebling SW, Farrar CR, Prime MB, Shevitz DW. Damage identification and health monitoring on structural and mechanical systems from changes in their vibration characteristics: a literature review. Report LA-13070-MS, Los Alamos National Laboratory 1996; USA.

[9] Salawu OS. Detection of structural damage through changes in frequency: a review. Eng Struct 1997; 19(9): 718.

[10] Farrar CR, Baker WE, Bell TM, *et al*. Dynamic characterization and damage detection in the I-40 bridge over the Rio Grande. Report LA-12767-MS, Los Alamos National Laboratory 1994; USA.

[11] Pandey AK, Biswas M, Samman M. Damage detection from changes in curvature mode shapes. J Sound Vibrat 1991; 145(2): 321-332.

[12] Doebling SW, Farrar CR. Statistical damage identification techniques applied to the I-40 Bridge over the Rio Grande River. Proceeding of the 16th IMAC 1998; 717-1724.

[13] Reynders E, De Roeck G. Measurement of modal curvatures using optical fiber strain sensors and application to damage identification using vibration monitoring. Proceeding of the 17th International Conference on Optical Fibre Sensors, SPIE, Bellingham, WA 2005; 1076-1079.

[14] Pandey AK, Biswas M. Damage detection in structures using changes in flexibility. J Sound Vibrat 1994; 169(1): 3-17.

[15] Zhang Z, Aktan AE. The damage indices for constructed facilities. Proceeding of the 13 IMAC 1995: 1520-1529.

[16] Cornwell PJ, Doebling SW, Farrar CR. Application of the strain energy damage detection method to plate-like structures. J Sound Vibrat 1999; 224(2): 359-374.

[17] Alvandi A, Cremona C. Reliability of bridge integrity assessment by dynamic testing Proceeding of the 1st European workshop on Structural Health Monitoring, Paris, France 2002; 125-137.

[18] Li Huajun, Yang Hezhen, Hu S-L James. Modal strain energy decomposition method for damage localization in 3D frame structures. J Eng Mechan ASCE, 2006; (132): 941-951.

[19] Hu S-L James, Wang Shuqing, Li Huajun. Cross-modal strain energy method for estimating damage severity. J Eng Mechan ASCE 2006; (132): 429-437.

[20] Allemang RJ, Brown DL. A correlation coefficient for modal vector analysis. Proceeding of the 1st IMAC, Orlando, Florida, USA, 1982: 110-116.

[21] Rudenko OV. Giant nonlinearities in structurally inhomogeneous media and the fundamentals of nonlinear acoustic diagnostic techniques. Physics-Uspekhi 2006; 49 (1): 69-87.

[22] CHBDC. Canadian Highway Bridge Design Code. A National Standard of Canada CAN/CSA-S6-00 2000.

[23] Jolin M, Bastien J, Perron JP. Load test and assessment of a concrete bridge: case study. Proceedings of the Second Workshop on Life Prediction, Paris, France; Edited by Naus DJ, (RILEM Publications) 2003.

[24] ANSYS. Robust Simulation and Analysis Software, ANSYS : Element Description, Solid45, http://www.ansys.com/; release 11 2007.

[25] Farrar CR, Duffey TA, Cornwell PJ, Doebling SW. Excitation methods for bridge structures. Proceeding of the 17th International Modal Analysis Conference Kissimmee, FL 1999.

[26] Cremona C, Barbosa FS, Alvandi A. Modal identification under ambient excitation: application to bridge monitoring. Mécanique Industries 2003; 4: 259-271.

[27] Brincker R, Zhang L, Andersen P. Modal identification from ambient responses using frequency domain decomposition. Proceeding of the 18th IMAC, San Antonia, Texas, USA 2000; 26-32.

[28] Brincker R, Zhang L, Andersen P. Modal identification of output-only systems using frequency domain decomposition. Smart Mater Struct 2001; (10): 441-445.

Received: April 17, 2008 Revised: May 5, 2008 Accepted: May 14, 2008